Low-temperature transport anomaly in the magnetoresistive compound $(La_{0.5}Pr_{0.2})Ba_{0.3}MnO_3$

D. S. Rana, J. H. Markna, R. N. Parmar, and D. G. Kuberkar

Department of Physics, Saurashtra University, Rajkot—360 005, India

P. Raychaudhuri, J. John, and S. K. Malik*

Tata Institute of Fundamental Research, Mumbai—400 005, India

Electronic and magnetoresistive properties of $(La_{0.5}Pr_{0.2})Ba_{0.3}MnO_3$ (ABO_3 type) compound, having a large size-disorder at the A-site, have been studied in both polycrystalline bulk as well as in epitaxial thin-film forms. Both these forms of the sample display a resistivity minimum at a temperature (T_{min}) of ~45 K; T_{min} shifts to higher temperatures on application of magnetic fields. Considering various possibilities, such as a grain boundary effect, Kondo scattering, and electron-electron (e-e) scattering for the cause of this resistivity minimum, we conclude that the minimum occurs due to e-e scattering caused by enhanced Coulombic interactions. A large size-disorder ~0.016 Å^2 in this compound is the major source of metallic disorder, resulting in the enhancement of Coulombic interactions.

For nearly the last decade, there has been extensive research on ABO_3-type manganites of the general formula $R_{1-x}A_xMnO_3$ ($R=$ rare earth trivalent cation, $A=$ divalent cation). In a certain critical range of divalent cation doping, tolerance factor, and size-disorder at the A-site, these compounds exhibit simultaneous insulator-metal (I-M) transition at a temperature T_p and paramagnetic-ferromagnetic transition at a temperature T_C, along with a colossal magnetoresistance in the vicinity of T_p.[1–3] The electronic transport, above and below the I-M transition temperature, has been studied extensively and is well understood [for a review, see Refs. 1 and 2]. The low-temperature electronic transport in some manganites presents a feature of weak insulating/semiconducting behavior, which results in a resistivity minimum in the metallic region, and the opinion of its cause is divided.[4–7] In $La_{0.5}Pb_{0.5}MnO_3$ compound, the resistivity minimum is ascribed to grain boundary localization,[4] while in Sr^{2+}- and Ca^{2+}-doped compounds, the same has been attributed to variable range hopping[5] and to electron-electron (e-e) scattering[6,7] due to potential fluctuation in the cores of trivalent and divalent cations. The e-e scattering arises from enhanced Coulombic interactions (CI), which are present in disordered metallic systems. Here, the source of disorder may be defects, impurities, and other temperature-dependent scattering phenomena.

The Ba^{2+} (~1.47 Å)-doped manganite compounds present a large size-disorder at the A-site, resulting in various local structural distortions, which cause electron localization and grain boundary localization.[8] There are few reports on Ba-based compounds exhibiting a low-temperature resistivity minimum either in polycrystalline or single-crystal forms, and the cause of such a resistivity minimum in these compounds has not been adequately explored.[9,10] In addition, in manganites, comparison of transport properties of epitaxial thin-film or single-crystal structural forms with polycrystalline forms is the most appropriate way to determine and distinguish the role of grain boundaries in electronic transport. The epitaxial thin films display a much reduced grain boundary effect on the transport properties as compared to bulk

polycrystalline samples. Therefore, to elucidate whether the low-temperature resistivity minimum is an intrinsic property or arises from grain boundaries, we have synthesized the compound $(La_{0.5}Pr_{0.2})Ba_{0.3}MnO_3$ (average A-site cationic size ~1.285 Å and a large $\sigma^2 \sim 0.015$ Å^2) in polycrystalline bulk as well as epitaxial thin-film forms. Here, the epitaxial thin films with varying thickness have been synthesized to probe the low-temperature transport anomalies. In this article, we show the role of size-disorder at the A-site in the occurrence of low-temperature resistivity minimum in such compounds.

A bulk polycrystalline sample of $(La_{0.5}Pr_{0.2})Ba_{0.3}MnO_3$ was synthesized by mixing the constituent oxides and carbonates in stoichiometric proportions and calcinating the mixture at 950 °C for 24 h. The powder was then ground, pelletized, and sintered several times in the temperature range of 1100–1350 °C. Thin films with thicknesses of 200, 100, and 50 nm were deposited on single-crystal $LaAlO_3$ (100) substrate by pulsed-laser deposition technique using a KrF excimer laser. The substrate-to-target distance was kept at 4.2 cm with substrate heater temperature at 830 °C. The O_2 partial pressure was maintained at 400 mTorr. Phase purity and the structure of the samples were studied using x-ray diffraction (XRD). Electrical resistivity and magnetoresistance were measured using dc four-probe method (PPMS, Quantum Design) while the magnetization measurements were performed on a superconducting quantum interference device magnetometer (MPMS, Quantum Design).

The XRD pattern of the $(La_{0.5}Pr_{0.2})Ba_{0.3}MnO_3$ bulk sample revealed that this is a single-phase compound crystallizing in a distorted orthorhombic structure (space group *Pnma*, No. 62) with lattice parameters determined as $a=5.512(2)$ Å, $b=7.791(2)$ Å, and $c=5.548(2)$ Å. The thin-film samples were also indexed to be single phase and (101) oriented, with nearly the same lattice parameters as the bulk sample. The surface morphology of thin films was studied using atomic force microscopy (AFM). A typical AFM picture for 200 nm thin film is shown in Fig. 1. It shows the
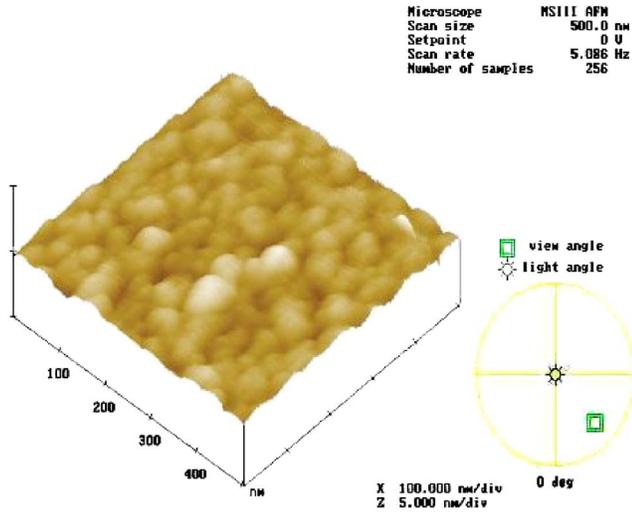
FIG. 1. AFM micrograph of $(La_{0.5}Pr_{0.2})Ba_{0.3}MnO_3$ 200 nm thin film.

FIG. 2. Resistivity vs temperature plots for (a) bulk and (b) thin film (thickness $\sim$ 200 nm) of $(La_{0.5}Pr_{0.2})Ba_{0.3}MnO_3$ compound. Inset in (b) shows the magnified part of the low-temperature resistivity.

surface roughness of $\sim$2–3 nm and a particle size of $\sim$6–7 nm, which is a very moderate morphology typical for epitaxial and homogeneous manganite thin films. Figures 2(a) and 2(b) show resistivity versus temperature plots of the $(La_{0.5}Pr_{0.2})Ba_{0.3}MnO_3$ bulk polycrystalline and thin film of 200 nm, respectively, in different applied magnetic fields (for the sake of brevity, resistivity versus temperature of 100 and 50 nm thin films are not shown). In the bulk sample, the I-M transition occurs around a temperature of 173 K and the resistivity minimum around a temperature (T_{min}) of 50 K. The resistivity minimum in the thin-film (200 nm) sample is not clearly visible in the plot due to the large value of peak resistivity. Therefore, to emphasize the minima, a magnified part of the low-temperature resistivity is shown as an inset in Fig. 2(b). In the absence of a magnetic field, the bulk and thin-film samples of $(La_{0.5}Pr_{0.2})Ba_{0.3}MnO_3$ show T_{min} in the vicinity of 45 K (Table I). This minimum shifts to higher temperatures in applied magnetic fields. We notice that the I-M transition temperature in thin films occur around a temperature of 210 K, which is higher than the temperature for
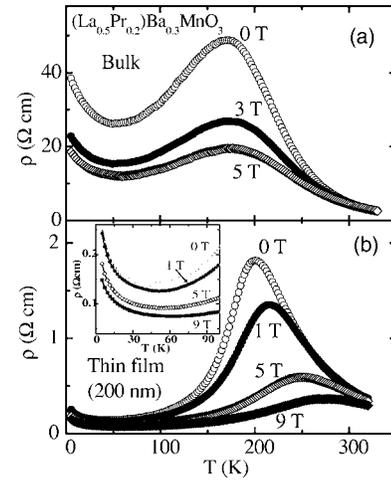
the same in bulk (173 K). This difference has been attributed to factors such as the grain boundary effect, oxygen deficiency, phase separation near T_C, etc.

Various possible causes for the low-temperature resistivity minimum in the presently studied $(La_{0.5}Pr_{0.2})Ba_{0.3}MnO_3$ samples are considered. These include the grain boundary, phase-separation, the Kondo effect, and electron-electron localization.[11,12] A resistivity minimum due to the Kondo effect arises due to scattering from a magnetic impurity in a nonmagnetic lattice. The present sample is ferromagnetic at 205 K (Fig. 4), with no detectable impurity. In addition, the resistivity minimum caused due to grain boundaries, phase separation, and the Kondo effect should dissolve on the application of magnetic fields.[11,12] However, as seen in Fig. 2, for both the bulk and the thin-film (200 nm) samples, application of a magnetic field only suppresses the magnitude of resistivity but causes no impact on the resistivity minimum. A moderately smooth surface morphology of the thin films indicates the homogeneous structure of the thin films. This is striking evidence against the grain boundary and phase sepa-

TABLE I. Parameters obtained from fitting the resistivity data to the equation $\rho = \{1/(\sigma_0 + BT^{1/2})\} + \rho_n T^n$. For definition of parameters, see text.

Thin-film samples (nm)	Magnetic field (T)	T_{min} (K)	σ_0 (Ω^{-1} cm^{-1})	B (Ω cm K$^{1/2}$)$^{-1}$	ρ_n (10^{-5} Ω cm/K^n)	n	χ^2 (10^{-6})
200	0	45	1.69	1.02	0.41	2.25	1.7
	1	48	1.75	1.07	0.20	2.24	1.9
	5	53	2.12	1.52	0.69	1.95	0.2
	9	61	2.85	1.73	0.82	1.82	0.07
100	0	40	4.73	0.46	0.09	2.48	0.3
	1	42	4.67	0.50	0.17	2.35	0.2
	5	46	4.87	0.62	0.35	2.11	0.08
50	0	40	3.83	0.64	0.23	2.38	0.8
	5	49	3.93	0.86	0.93	1.93	0.08

ration or the Kondo effect being a cause of such a resistivity minimum.

The electron-electron scattering due to Coulombic interactions between the charge carriers is the most likely cause of the resistivity minimum.[11,12] Such a kind of scattering is possible when the low-temperature resistivity is more than the Mott's maximum limit of metallic resistivity of ~ 10 mΩ cm.[11,12] In our thin-film samples, the resistivity is quite above this limit, and hence the e-e elastic scattering is quite plausible. The resistivity in the metallic region is due to various electron-phonon and electron-magnon inelastic scattering processes. At low temperature, e-e elastic scattering dominates and, therefore, the resistivity may be defined by summing the elastic and the inelastic scattering terms, as

$$\rho = \rho_{\text{elastic}} + \rho_{\text{inelastic}}. \quad (1)$$

The low-temperature correction (e-e scattering) to the resistivity, given by ρ_{elastic}, is quantified[11,12] as $\rho_{\text{elastic}} = 1/(\sigma_0 + BT^{1/2})$, where σ_0 is the residual conductivity and B is a constant that depicts the depth of the resistivity minimum. The inelastic scattering term is given by a power law, $\rho_{\text{inelastic}} = \rho_n T^n$. With these definitions, Eq. (1) becomes

$$\rho = \frac{1}{\sigma_0 + BT^{1/2}} + \rho_n T^n. \quad (2)$$

The elastic term [first term in Eq. (2)] increases with decreasing temperature, while the inelastic scattering term [second term in Eq. (2)] decreases with decreasing temperature. Therefore, the temperature-dependent interplay of these two scattering processes results in a resistivity minimum. As shown in Fig. 3, the fits to low-temperature resistivity for all the thin-film samples to Eq. (2) reveal an excellent agreement between experimental data and theoretical assumptions. This is evident from the very low χ^2 (goodness of the fit) values given in Table I. All the parameters obtained from the fits are given in Table I. The parameter n in the inelastic term is ~ 2.5 for resistivity fits in the absence of a magnetic field and decreases on the application of a magnetic field.

It may be seen from Table I that T_{min} shifts to higher values as the applied magnetic field increases. For instance, in 200 nm thin film, T_{min} increases from 45 K in 0 T to 61 K in 9 T. This is consistent with the theoretical predictions of an increase in T_{min} with increasing magnetic field. This may be understood in terms of magnetic field induced suppression of inelastic scattering, whereas the elastic term is hardly affected by the magnetic field. This is also evident from the fact the value of inelastic scattering exponent (n) decreases with applied field. Among other terms, B increases as the field increases and it signifies the depth of the minima. The importance of B may be understood as the contribution to CI, resulting in scattering of electrons. The variation of T_{min} with applied field, as predicted theoretically, is a point in support of CI being the cause of the resistivity minimum.

Below the resistivity minimum, the decreased electron mobility with increasing e-e scattering may result in a glassy state. To study this, the zero-field-cooled (ZFC) and field-cooled (FC) magnetization measurements on $(\text{La}_{0.5}\text{Pr}_{0.2})\text{Ba}_{0.3}\text{MnO}_3$ thin film (200 nm) were carried out in
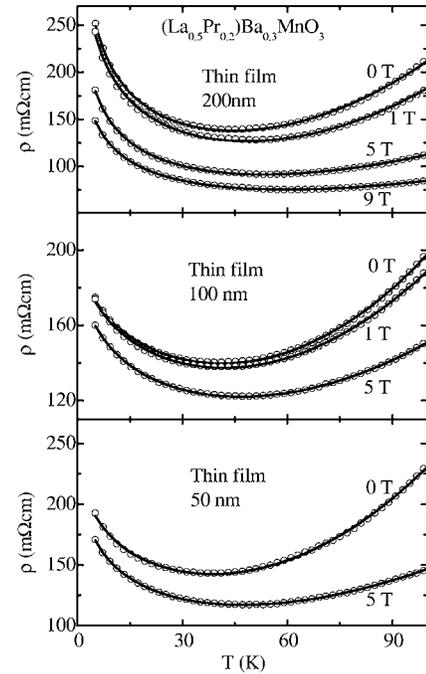

FIG. 3. Low-temperature resistivity fits to electron-electron scattering law for $(\text{La}_{0.5}\text{Pr}_{0.2})\text{Ba}_{0.3}\text{MnO}_3$ thin-film samples with thicknesses of ~ 200, 100, and 50 nm. The symbols are the experimental data and the solid curves are the theoretical fits.

the field of 200 Oe in the temperature range of 250–5 K, and the results are shown in Fig. 4. The T_C of the thin films is found to be ~ 205 K, which agrees well with the T_p of thin films, thus indicating the homogeneous structure of thin films. An important point to note is the bifurcation of the ZFC and FC curves. This bifurcation is small above 40 K, whereas it suddenly increases below this temperature. The increased bifurcation of M_{ZFC} and M_{FC} points towards a glassy state below T_{min}, which is consistent with the enhanced resistivity below T_{min}.

Figure 5 shows the typical magnetoresistance (MR%) versus magnetic field (H) isotherms at various temperatures for $(\text{La}_{0.5}\text{Pr}_{0.2})\text{Ba}_{0.3}\text{MnO}_3$ bulk and thin-film (200 nm) samples. For comparison of low-temperature MR behavior of bulk and all the thin-film samples, the MR isotherms, at 5 K, are plotted separately in Fig. 6. It is seen that, near the I-M
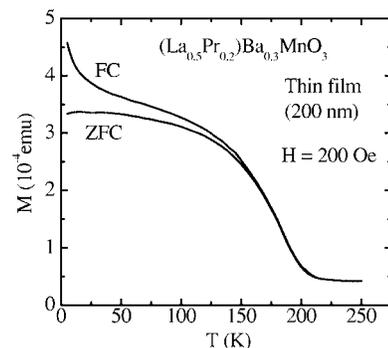

FIG. 4. ZFC and FC magnetization vs temperature plots for $(\text{La}_{0.5}\text{Pr}_{0.2})\text{Ba}_{0.3}\text{MnO}_3$ thin film in a field of 200 Oe.
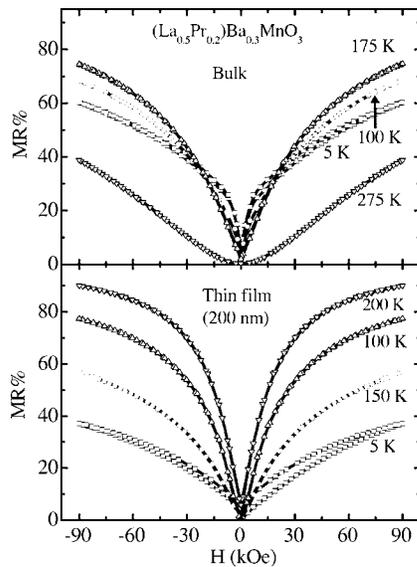
FIG. 5. MR% vs magnetic field isotherms for $(La_{0.5}Pr_{0.2})Ba_{0.3}MnO_3$ bulk and thin film (200 nm).

FIG. 6. MR% vs magnetic field isotherms for $(La_{0.5}Pr_{0.2})Ba_{0.3}MnO_3$ bulk and all the thin films at a temperature of 5 K.

transition, the MR is $\sim$75% for the bulk sample and $\sim$90% for the thin-film samples. In the bulk sample, at 5 K, the total MR% decreases to $\sim$60%, but the low-field ($<$1 T) MR of about 25% may be attributed to the intergranular spin-polarized tunneling (SPT) of carriers.[13] On the other hand, the thin films exhibit a MR of $<$30% at 5 K, signifying the absence of intergrain SPT. However, the high-field MR behavior is almost the same for both the samples. Thus, it is noted that, at low temperatures, the grain boundary has a significant contribution to the electrical resistivity of the bulk sample but not to that of the thin films.[14] Hence, the disparity in low-temperature MR behavior of the bulk and thin-film samples strongly supports our finding that the low-temperature minimum does not have its origin in grain boundaries.

From the above discussion, the e-e scattering seems to be cause of the resistivity minimum in $(La_{0.5}Pr_{0.2})Ba_{0.3}MnO_3$. The e-e scattering arises from some metallic disorder.[11,12] O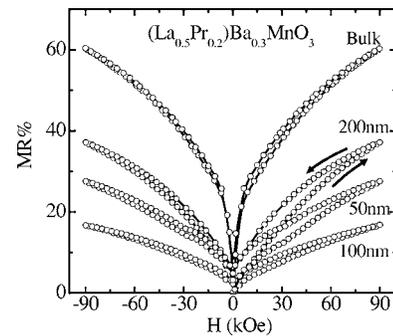ne source of such a disorder is the potential difference due to cores of trivalent and divalent cations and the other is the structural distortion caused by large size-disorder at the A-site. The present sample has a large size-disorder, resulting in local structural distortion via random displacement of oxygen ion from its actual crystallographic position. These distortions are of both the Jahn-Teller and the non-Jahn-Teller type and are a major source of disorder in this system.

In summary, we have studied the low-temperature transport anomalies in $(La_{0.5}Pr_{0.2})Ba_{0.3}MnO_3$ polycrystalline bulk and thin-film samples. The intent of this study is to elucidate whether the low-temperature resistivity minimum in this Ba-based sample is an intrinsic crystal structure property or is a grain boundary property. After appropriate modeling of low-temperature resistivity data of the thin-film samples, we conclude that the low-temperature resistivity minimum in Ba-based compounds is an intrinsic property. The application of magnetic field shifts T_{min} to higher temperatures. The e-e scattering, as a result of Coulombic interactions, is responsible for the resistivity minimum. The origin of such a behavior lies in the large size-disorder at the A-site, which causes the local structural distortions and is a major source of disorder in this low-temperature metallic regime.

*Electronic address: skm@tifr.res.in

[1] A. P. Ramirez, J. Phys.: Condens. Matter **9**, 8171 (1997).

[2] E. Dagotto, T. Hotta, and A. Moreo, Phys. Rep. **344**, 1 (2001).

[3] H. Y. Hwang, S.-W. Cheong, P. G. Radaelli, M. Marezio, and B. Batlogg, Phys. Rev. Lett. **75**, 914 (1995).

[4] E. Rosenberg, M. Auslender, I. Felner, and G. Gorodetsky, J. Appl. Phys. **88**, 2578 (2000).

[5] P. Raychaudhuri et al., cond-mat/9805320 (unpublished).

[6] M. Auslender, A. E. Karkin, E. Rosenberg, and G. Gorodetsky, J. Appl. Phys. **89**, 6639 (2001).

[7] D. Kumar, J. Sankar, J. Narayan, Rajiv K. Singh, and A. K. Majumdar, Phys. Rev. B **65**, 094407 (2002).

[8] L. M. Rodriguez-Martinez and J. P. Attfield, Phys. Rev. B **58**, 2426 (1998).

[9] A. Maignan, C. Martin, M. Hervieu, B. Raveau, and J. Hejt-manek, Solid State Commun. **107**, 363 (1998).

[10] O. Toulemonde, F. Studer, A. Llobet, L. Ranno, A. Maignan, E. Pollert, M. Nevriva, E. Pellegrin, N. B. Brooks, and J. Goedkoop, J. Magn. Magn. Mater. **190**, 307 (1998).

[11] B. L. Altshuler and A. G. Aronov, in Electron-Electron Interactions in Disordered Systems, edited by A. L. Efros and M. Pollak (North Holland, Amsterdam, 1985).

[12] P. A. Lee and T. V. Ramakrishnan, Rev. Mod. Phys. **57**, 287 (1985).

[13] H. Y. Hwang, S.-W Cheog, N. P. Ong, and B. Batlogg, Phys. Rev. Lett. **77**, 2041 (1996).

[14] P. Raychaudhuri, K. Sheshadri, S. Bandyopadhyay, P. Ayyub, A. K. Nigam, R. Pinto, S. Chaudhuri, and S. B. Roy, Phys. Rev. B **59**, 13919 (1999).